 

# Configuration of Adsorbed Phases and Their Evolution to Absorbent States in the $CH_4$–$O_2$ Catalytic Reaction

**Joaquín Cortés*** **and Eliana Valencia**

Facultad de Ciencias Físicas y Matemáticas, Universidad de Chile, Casilla 2777, Santiago, Chile

Received July 24, 2008; E-mail: jcortes@dqb.uchile.cl

Through kinetic Monte Carlo simulations of a catalytic reaction with a complex mechanism, such as the catalytic oxidation of methane, it is shown that the temporal evolution of the adsorbed phase to absorbent states is interpreted by an exponential decay of production. This semiempirical law, which has been used previously for systems with simple mechanisms, describes reactive and absorbent states and is in agreement with the results of the phase diagram. Substrates corresponding to square, hexagonal, and eight-coordination lattices are analyzed. In the first case it is shown that for most of the phase diagram the absorbent configuration of the adsorbed phase complies with the checkerboard structure found by Brosilow and Ziff in the case of a simple mechanism for the CO–NO reaction over a square lattice.

Over the last decades great progress has been made in the knowledge of superficial catalytic reactions. This has been due on the one hand to modern laboratory techniques and on the other to a better understanding of the behavior of irreversible dynamic systems of which superficial reactions are an example. These kinds of systems have called the joint attention of chemists because of their applications in catalysis and of physicists because they are good examples of nonequilibrium models that show interesting complex phenomena such as oscillations, kinetics phase transitions, hysteresis, chaos, dissipative structures, etc.[1]

On the other hand, the existence of absorbent states of the surface configuration at which the reaction stops working is of great theoretical and certainly practical interest. Among these states we may mention those that ben-Avraham et al.[2] called saturated, in which the catalytic process ends because a surface species covers the substrate completely, as in the case of oxygen or carbon monoxide in the classic ZGB model,[3] to distinguish them from poisoned states in which an outside species succeeds in destroying the catalytic character of the substrate. Other situations can be mentioned in which some structures of the surface configuration succeed in stopping the reaction. That is the case, for example, of what we may call the checkerboard effect observed in a simplified mechanism of the CO–NO reaction, where the adsorbed phase tends inevitably to a particular absorbent state, as shown theoretically by Brosilow and Ziff[4] and Meng, Weinberg, and Evans,[5] and confirmed from results obtained in Monte Carlo (MC) simulations on uniform two-dimensional surfaces[4–6] and by our group on three-dimensional fractals.[7]

In spite of its importance, this phenomenon has not been studied sufficiently except for simple systems. Aspects such as the temporal evolution of the active surface phase until the final collapse of the process have not been determined in highly complex systems such as the combustion of hydrocarbons. These kinds of systems, important in power generation and in pollution studies, have been shifting the interest that research on the $CO$–$O_2$ and CO–NO reactions had for many years because of their importance in catalytic converters of automobiles.[8]

A motivation of the present work has to do with the fact that the evolution of activity to absorbent states is also of great interest in relation to the phenomenon of catalyst stabilization and deactivation, as has been mentioned in the case of the CO–NO reaction[9] and has recently been studied in greater detail in the $CH_4$–$O_2$ reaction.[10] In the latter case in our laboratory we are currently studying, based on our simulations of absorbent states and through experiments and Monte Carlo simulations, the deactivation phenomenon and its relation with the structure of the catalyst's surface. We have seen, for example in a supported catalyst, that the difference in the decreasing evolution rate of the reaction's activity in sectors that coexist on the surface and have different crystallinity may be an explanation of the catalyst's deactivation seen in the experiment.

These aspects will be analyzed in this paper in the case of a complex system, the catalytic combustion of methane, using a Monte Carlo simulation model that was developed for the first time for this system in a recent paper by our group.[11] Recently, Zhdanov et al. published other interesting MC simulation of the $CH_4$–$O_2$ reaction.[12]

## Experimental and Theoretical Background

**The Catalytic Combustion of Methane.** The oxidation of methane ($CH_4$–$O_2$ reaction) is a complex system of great interest in current literature.[13] In recent years a large number of papers on this interesting reaction have appeared because methane is a well-known greenhouse gas and the most stable and abundant alkane. The combustion of hydrocarbons, of great importance in power generation, occurs at sufficiently high temperatures to favor thermodynamically the formation of nitrogen oxides, $NO_x$, contributing to the pollution problem. This explains the interest in carrying out these reactions catalytically, usually over noble metals or their oxides, usually supported, lowering dramatically the temperature required for the process.

Published on the web June 12, 2009; doi:10.1246/bcsj.82.683

1) $O_2(g) + * \xleftrightarrow{K_1} O_2*$

2) $O_2* + * \xrightarrow{k_2} 2O*$

3) $CH_4(g) + * \xleftrightarrow{K_3} CH_4^*$

4) $CH_4^* + O* \xrightarrow{k_4} CH_3^* + OH*$

4 a) $CH_3^* + O* \longrightarrow CH_2^* + OH*$

4 b) $CH_2^* + O* \longrightarrow CH^* + OH*$

4 c) $CH^* + 2O* \longrightarrow CO^* + OH*$

4 d) $CO* + O* \longrightarrow CO_2^*$

4 e) $CO_2^* + O* \longrightarrow CO_3^*$

5) $2OH* \xleftrightarrow{K_5} H_2O(g) + O* + *$

6) $CO_2* \xrightarrow{k_6} CO_2(g) + *$

7) $CO_3* \xrightarrow{k_7} CO_2(g) + O*$

**Scheme 1.** Kinetic mechanism for the combustion of $CH_4$.

**Table 1.** Kinetic and Thermodynamic Parameters Used in the MC Simulations Defined in Scheme 1[a)]

| $K_1$ | $k_2$ | $K_3$ | $k_4$ | $K_5$ | $k_6$ |
|---|---|---|---|---|---|
| 0.1 $Torr^{-1}$ | $200k_1$ | 3 $Torr^{-1}$ | $0.05k_{-3}$ | 0.084 $Torr^{-1}$ | $k_6 = k_7 = 50k_1$ |

a) $K_i = k_i/k_{-i}$, $k_i$ = kinetic constant for the adsorption of $i$ (eq 2); $k_{-i}$ = kinetic constant for the desorption of $i$ ($i = 1$, 3, and 5) (Ref. 11).

In spite of the large amount of experimental work done over the last few years on the $CH_4$–$O_2$ reaction, the same has not happened with the theoretical interpretation of the microscopic characteristics of the reaction mechanism. Although there seems to be agreement that the reaction takes place by the direct interaction of the reactants with the oxygen of the network via a mechanism of the Mars–van Krevelen (MK) type,[14] the only complete mechanism that is found in the literature, almost certainly because of the system's complexity, is an interpretation of the Langmuir–Hinshelwood (LH) type, reported by Iglesia et al.[15] in the case of a $PdO_x/ZrO_2$ surface at low temperature. Scheme 1 shows the details of that mechanism, including fast steps (4a–4e) that we have assumed in our MC simulations of the process. In those reactions the asterisks represent an oxygen vacancy on the $PdO_x$ surface corresponding to Pd sites, necessary for the linear adsorption of $CH_4$ and $O_2$ from the gas-phase and for the dissociation of $O_2$* adsorbed on the surface. The mechanism assumes the existence of some irreversible stages and others under quasi-equilibrium conditions. It is interesting to note that the above LH scheme is indistinguishable in the simulations from one of the MK type, in agreement with the comment of Iglesia et al.[15] in their original paper that "this elementary step sequence resembles the Mars–van Krevelen reduction–oxidation pathways."

**Kinetic Monte Carlo Simulations.** The kinetic Monte Carlo (kMC) algorithm developed in this paper is similar to others used previously by our group for various reactions, both abstract and real, such as the oxidation of CO or the reduction of NO by CO,[16] and to that reported recently by our group[11] for the $CH_4$–$O_2$ reaction with which this paper deals. The substrates used in the simulations were a uniform surface made of sites located in an $L \times L$ square lattice with periodic boundary conditions ($L = 50$) with near neighbors nn ($N = 4$) and nn + next nearest neighbors nnn ($N = 8$). The case of a hexagonal lattice ($N = 6$) with periodic boundary conditions has also been considered. The simulation algorithm begins by choosing an event of the mechanism (adsorption, desorption, dissociation, or reaction) according to the probability $p_i$ of the event defined by

$$p_i = k_i \Big/ \sum k_i \tag{1}$$

where $k_i$ corresponds to the rate constant of step $i$ of the mechanism. In the case of adsorption, it was calculated from the collision of molecules with a solid surface (effusion) expression:[17]

$$k_i(\text{ads}) = S_i\sigma(2\pi M_i RT)^{-1/2} \tag{2}$$

where $M_i$ is the molar mass of $i$, $S_i$ is the corresponding sticking coefficient ($S_i = 1$ in this case), and the coefficient $\sigma$ is the area occupied by 1 mol of superficial metal atoms ($4.74*10^8$ $cm^2$ $mol^{-1}$ for Pd). The remaining $k_i$ constants used in the paper were chosen using criteria similar to those of the previous paper.[11] For that purpose, and since in the literature there are no reliable values available for most of the steps of the mechanism of Scheme 1, the rate and equilibrium constants and some relations between constants shown in Table 1 were chosen, whose magnitudes are of a reasonable order in relation to values of typical reactions found experimentally. In this way the remaining kinetics constants required can be obtained. For example, from the values of the equilibrium constants of Table 1 chosen for reactions 1 and 3 for the mechanism, the oxygen and methane desorption constants are obtained using eq 2 for the adsorption constants and the well-known relation $K_i = k_i/k_{-1}$. The MC algorithm begins with the selection of the event. If it corresponds to the adsorption of $O_2$, a site is chosen randomly on the surface, and if it is vacant a molecular oxygen particle, $O_2$*, will remain adsorbed. If the site is occupied, the attempt is ended. If the adsorption of $CH_4$ is chosen, the procedure is completely analogous, and a $CH_4$* particle remains adsorbed. If the adsorption of $H_2O$ is chosen and the site is empty, the sites neighboring the original site are revised. If no O* particle is found, the attempt is ended. If one of the neighbors is occupied by O*, both sites are occupied by OH* particles. If there is more than one neighbor occupied by O*, one of them is chosen randomly.

If $O_2$ desorption is chosen, a surface site is selected randomly. If it is occupied by a particle different from $O_2$* or it is vacant, the attempt is ended. However, if it is occupied by an $O_2$* particle, desorption occurs and the particle is replaced by a vacant site. The procedure is analogous in the case of choosing the desorption of $CH_4$ and $CO_2$. In the case of the desorption of $CO_3$* the particle is replaced by an adsorbed atomic oxygen, O*, and a molecule of $CO_2$ leaves the surface.

In the case of chemical reaction events that involve two reactant particles, a site of the surface is first chosen randomly. If it is occupied by a particle corresponding to one of the reactants, a

neighboring site is then chosen randomly next to the first site. If the latter is occupied by the other particle of the same reaction, the event is successful and the corresponding reaction is carried out. For example, if the first particle is $CH_4$* and the second is O*, a particle of $CH_3$* remains in the first site and one of OH* in the second, and if both particles are OH*, one molecule of $H_2O$ leaves the surface and a particle of O* remains in the first site. If around $CH_3$* there was one or more O*, one or more of the fast reactions occur (reactions 4a–4e).

When the chosen event is the dissociation of $O_2$, a surface site is chosen randomly. If it is occupied by an $O_2$* particle, a neighboring site is chosen randomly next to the first site. If this is empty, dissociation occurs and a particle of O* is placed at each of the two previous sites. If the site is occupied, the attempt is ended. Since the mechanism considers that the abstraction reactions 4a–4e of a series of radicals with adsorbed atomic oxygen are instantaneous, it is necessary to review all the neighbors of both O* that have resulted in the dissociation. If some radical is found, the corresponding reaction takes place in a manner similar to the case of the chemical reaction event mentioned in the previous paragraph. If more than one radical is found, one of them is chosen randomly and the process goes on as above. It is also assumed that the neighbors are equivalent. Computing time was measured in Monte Carlo Steps (MCS), defined as a number of attempts equal to the number of sites in the substrate.

**Evolution of the System to an Absorbent State.** The central theme of this paper is related to an aspect that is of basic interest in the study of the evolution of non-equilibrium systems to absorbent states, as well as of applied importance in the loss of activity when a reaction takes place on a catalytic surface. In this case, even though the phenomenon has not been studied in sufficient depth, several causes have been detected, such as sintering of the substrate which leads to a hyperbolic activity decay law[18] or to poisoning by particles that are chemisorbed irreversibly on the surface, in which case the system's activity shows an exponential time decay of the reaction.[19] Similar expressions between production $R_i$ of product $i$ of the reaction and time $t$ have been proposed by some theoretical groups that have attempted a microscopic visualization of the phenomenon, studying it also through computer simulations. Among the expressions that have been used to describe the system's temporal evolution we can mention the following:

$$R_i \approx \mathrm{e}^{-kt} \tag{3}$$

$$R_i \approx t^{-w} \tag{4}$$

$$R_i \approx (\ln \mathrm{t})^{-\sigma} \tag{5}$$

Parameters $k$, $w$, and $\sigma$, that describe the behavior of the system, are positive in the absorbent zones, so the above equations describe a decrease of $R_i$ until the system turns unproductive. Although the parameters in general can be considered of a semiempirical character, in some simple systems it is possible to determine theoretical values for them. For example, in the case of the monomer–monomer reaction ($A + B \rightarrow AB$), which has been studied extensively,[20,21] MC simulations give parameters $\sigma = 0.5$ and $w = 0.06$–$0.08$ when $y_A = 1/2$, characteristic of the model of Voter.[21] In this case the decay is associated with a "reactive coarsening" of domains of A and B where the reaction occurs only at the sites of the perimeters of isles of A and B. Another interesting example is the simplified mechanism of the CO–NO reaction mentioned earlier, for which Meng et al.[5] got for MC the values $w = 0.08$ and $\sigma = 0.69$ in the center of a pseudowindow where the value of parameter $k$ was cancelled, associating the slow poisoning with a "quasi-steady-state."

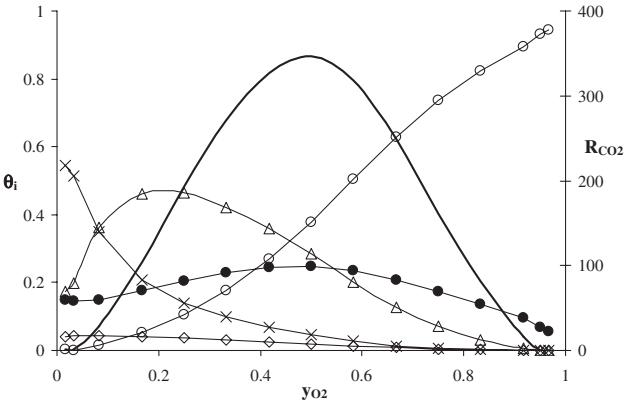


**Figure 1.** Production $(R_{CO_2}, y_{O_2})$ and phase diagram $(\theta_i, y_{O_2})$ at $T = 600$ K and $p_{O_2} + p_{CH_4} + p_{H_2O} = 60$ Torr, $p_{H_2O} = 1$ Torr, determined by MC simulations, for a hexagonal lattice in the steady state for the mechanism of Scheme 1 and the constants of Table 1. The lines have been drawn to guide the eyes. ○, O; ●, OH; ×, CH; △, $CH_4$; ◇, CO; —, $R_{CO_2}$.

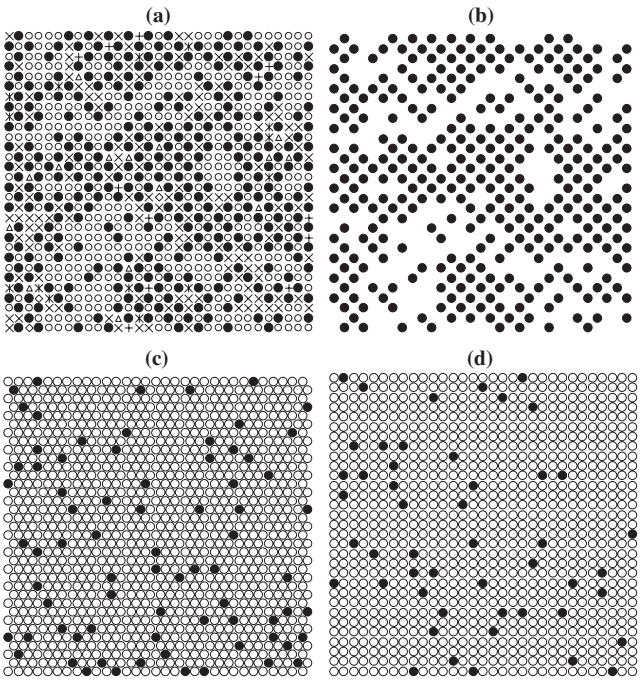


**Figure 2.** Snapshots of one part of the substrate's surface (under steady state conditions) for the catalytic combustion of methane, for the same conditions of Figure 1 and $N$ neighbors (a) a square lattice ($N = 4$), $p_{O_2} = 49$ Torr; (b) the same as (a) but for OH particles only; (c) hexagonal lattice ($N = 6$), $p_{O_2} = 57$ Torr; (d) square lattice ($N = 8$), $p_{O_2} = 58$ Torr. ○, O; ●, OH; ×, CH; △, $CH_4$; +, $CH_3$; ∗, $CH_2$; ◇, CO.

The aim of this work is to analyze the phenomenon of the deactivation that occurs under some circumstances in the catalytic $CH_4$–$O_2$ reaction, related to the structure of the catalytic surface, from the microscopic and theoretical standpoints, making use of our kMC model published recently for the first time for this reaction.[11] This allows the activity decay observed experimentally

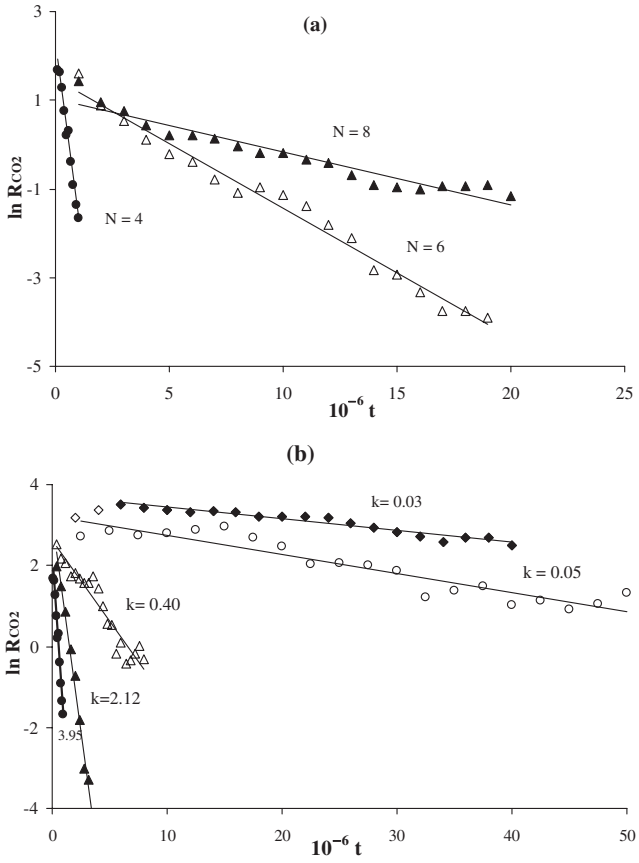


**Figure 3.** Graphs corresponding to eq 3 linearized (a) $N = 4$, $p_{O_2} = 57$ Torr; $N = 6$, $p_{O_2} = 58$ Torr, $N = 8$, $p_{O_2} = 58$ Torr; (b) the same as (a) for $N = 4$ at different $p_{O_2}$. $t$ is expressed in MCS and $R_{CO_2}$ in TON. ◆, $p_{O_2} = 49$ Torr; ○, $p_{O_2} = 51$ Torr; △, $p_{O_2} = 53$ Torr; ▲, $p_{O_2} = 7$ Torr; ●, $p_{O_2} = 57$ Torr.

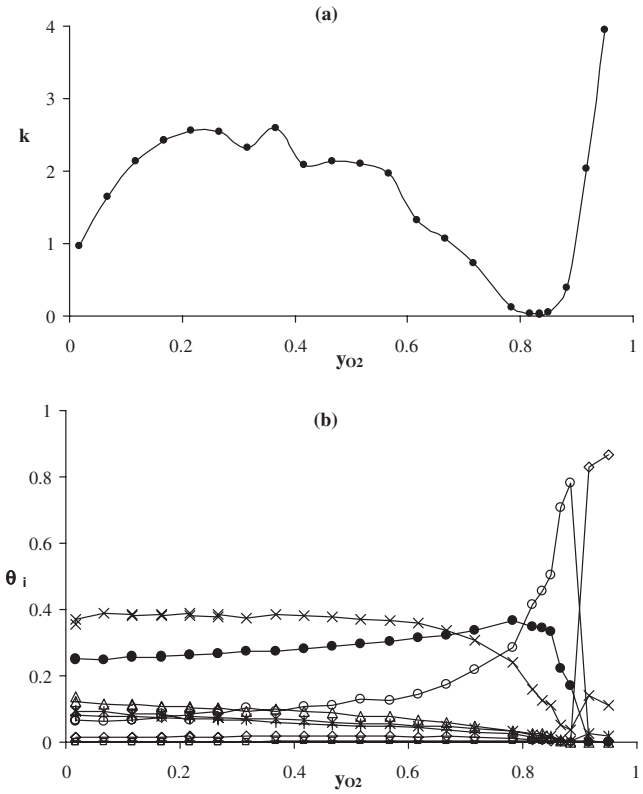


**Figure 4.** (a) Evolution rate $k$ to the absorbent state of eq 3 versus $y_{O_2}$ at $T = 600$ K and $N = 4$; (b) phase diagram ($\theta_i$, $y_{O_2}$) for $N = 4$ and $T = 600$ K. The lines have been drawn to guide the eyes. ○, O; ●, OH; ×, CH; △, $CH_4$; +, $CH_3$; ∗, $CH_2$; ◇, CO; □, $O_2$; –, S.

in our laboratory to be explained, as we will comment in some detail in the following section.

## Results and Discussion

The system consist of a gas-phase with a total pressure of 60 Torr, formed by a mixture of methane and oxygen and a small amount of water, in this case with a constant pressure equal to 1 Torr (1 Torr = 133.322 Pa) over the whole range of $y_{O_2}$, in contact with the catalyst.

Figure 1 shows the phase diagram and a $CO_2$ production diagram versus the oxygen concentration in the gas $y_{O_2}$ for the $CH_4$–$O_2$ reaction on a hexagonal lattice of active sites of the surface of the catalyst ($N = 6$). It is seen that the system has a wide window over nearly the whole range of $O_2$ concentrations, $y_{O_2}$, in the gas-phase, with absorbent zones only for high values of $y_{O_2}$. For the hexagonal and square lattices with $N = 8$ the diagrams are very similar, with a slightly higher activity for $N = 8$, not shown in the paper, over the whole extension of the window.

In the interesting case of a square lattice with the four nn of the site ($N = 4$), the system is poisoned for the whole range of $y_{O_2}$ concentrations, except apparently, as will be seen, in a very narrow sector of the diagram.

The production curves indicate, therefore, that it is possible to study the absorbent zone only over small intervals of $O_2$ concentration, except for $N = 4$. The latter is also the only case that presents the checkerboard effect, an example of which is shown in the snapshots of Figure 2a, where it is seen that the superficial OH* groups are located on every other diagonal of the lattice, because neighboring OH* groups react with one another. For greater clarity, Figure 2b shows the same part of the lattice including only the OH* species. The result is a diagonal lattice that isolates the rest of the particles from each other, poisoning the surface structurally. The diagonals can be cut by some different particle adsorbed on the surface. At the cutting points of the diagonals it is possible to see in the poisoned phase small sets of particles that do not react with one another. At high $y_{O_2}$ values the length of the diagonals decreases substantially, showing the existence of large O* isles within which isolated OH* particles surrounded by oxygen tend to be located, because they do not react with O*. This situation is rather similar to the case of $N = 8$ at high pressure, as shown in the snapshot of Figure 2d, where the absorbent phase consists of a sea of O* with some isolated OH* in it, in agreement with the phase diagram. A similar situation appears in the hexagonal lattice, where again the checkerboard effect cannot occur as shown in the snapshot of Figure 2c. The above is a consequence of the mechanism of Scheme 1, which indicates that the O* react with all the other particles except the OH* groups, and that the superficial particles do not react with one another, except the OH* groups.

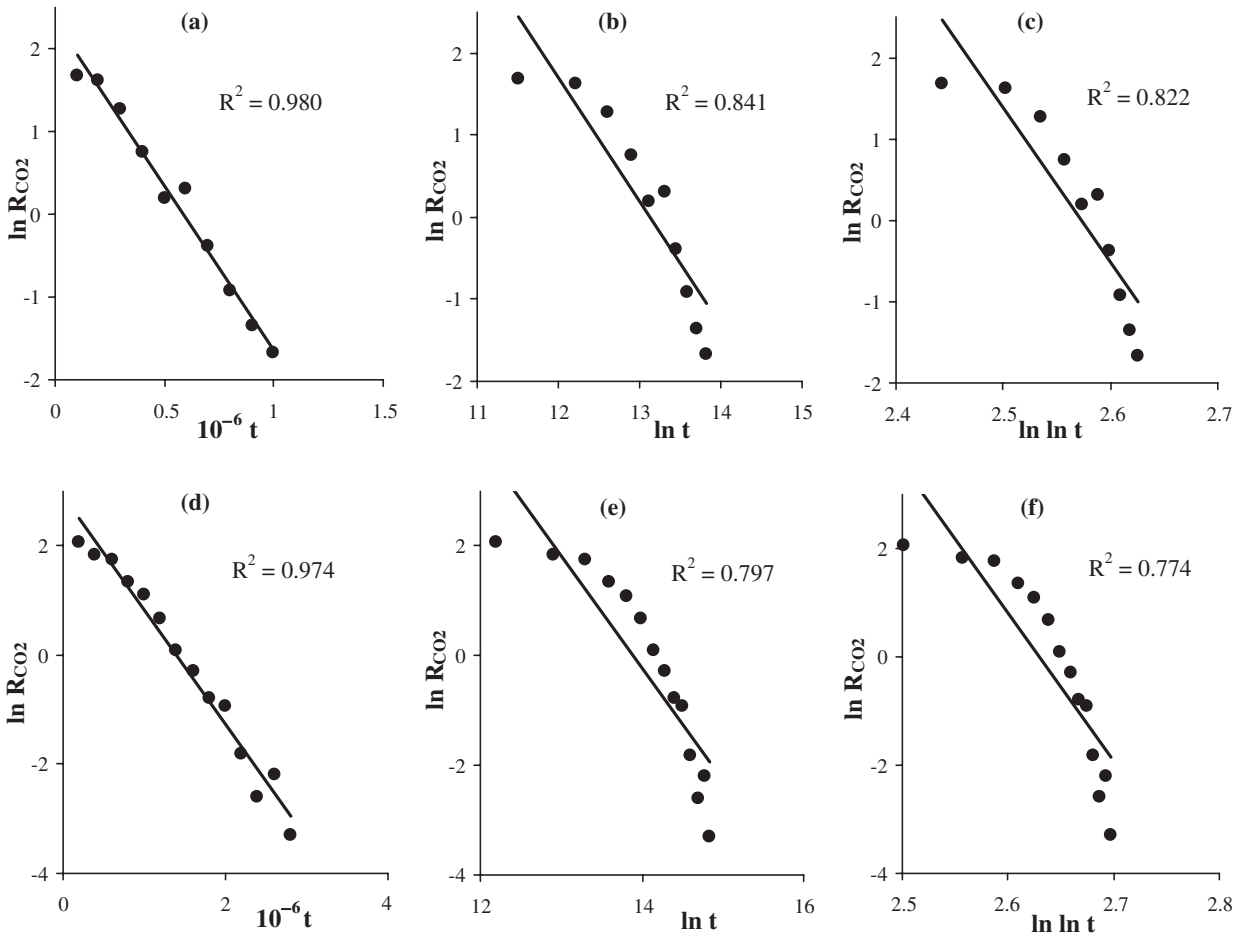


**Figure 5.** Graphs of eqs 3–5 linearized for the same set of simulated points for $T = 600$ K, $N = 4$ and (a, b, and c) $p_{O_2} = 57$ Torr, (d, e, and f) $p_{O_2} = 7$ Torr. $R^2$: least-square correlation coefficient. $t$ is expressed in MCS and $R_{CO_2}$ in TON.

At the same time, and complementing these studies, our laboratory is currently interested in the activity decay phenomenon seen experimentally under some circumstances in certain catalytic surface reactions. In a recent paper, for example, we have analyzed this phenomenon from the experimental standpoint and from that of the time decay of the activity in the case of the reduction of CO by NO reaction.[22] We are now studying this problem in detail under various experimental conditions in the $CH_4$–$O_2$ reaction catalyzed by palladium supported on silica. Our interpretation of the time decay of the activity in this case is based on the results reported in this paper. Experimentally we have shown that the catalytic substrate consists of supported particles whose heterogeneous surfaces have some sectors composed of square lattices. This can be studied by kMC simulating mixed surfaces on the computer, formed jointly, for example, by square and hexagonal sectors. Since the square zones become poisoned rather rapidly because of the checkerboard effect, which does not occur in the rest of the surface, it is possible to replicate qualitatively in the same simulations the strong initial decay seen experimentally, which turns smaller as reaction time goes by. The checkerboard effect, as already mentioned, had been reported for the CO–NO reaction, but it had not been related previously with the $CH_4$–$O_2$ reaction in the way shown, for example, in Figure 2.

The diagrams of Figure 3 show that the temporal evolution of $CO_2$ production can be described well by eq 3 in the three lattices studied ($N = 4$, 6, and 8) in zones where the system reaches an absorbent phase. The case of $N = 4$ is, as already commented, similar to the checkerboard structure found by Brosilow and Ziff for the case of a simple mechanism of the CO–NO reaction on a square lattice,[4–7] although in that system it is also possible to show theoretically the evolution to that absorbent state for a two-dimensional square lattice. On the other hand, in this case the system is absorbent over almost the whole range of $y_{O_2}$ concentrations, and the evolution to the absorbent state has a wide range of rates given by constant $k$ of eq 3, as seen in Figure 3b. Figure 4a shows for $N = 4$ the change of $k$ with the concentration of oxygen in the gas-phase, and Figure 4b the corresponding phase diagram. The values of $k$ represent a way of expressing the poisoning of the adsorbed phase, if it is seen that a steady state is reached for values of $k = 0$.

The phase diagram shows that the adsorbed phase is poisoned mainly with OH*, CH* and to a lower extent with other particles which like the latter react with oxygen. In the low and medium oxygen concentration zone the surface configuration is approximately constant in the phase diagram, and it corresponds to values of $k$ greater than one, with a

maximum approximately in the center of the diagram. This situation remains until a marked increase in superficial oxygen, due to the higher value of $y_{O_2}$, produces a substantial decrease of $CH_i$* particles, particularly CH*. It should be noted in eq 4c of Scheme 1 that the CH* particle requires two nn oxygen to react, and that accounts for the fact that the curve corresponding to $\theta_{CH}$ in the phase diagram decreases only when $\theta_O$ undergoes a substantial increase.

That situation leads, within the precision of our calculations, to a very narrow reactive window reflected in a decrease of $k$ until it almost cancels out in the zone where a maximum value of the OH* groups is seen. It is interesting to note that this situation and the values of the O*, CH*, and OH* coverage coincide approximately with those obtained at the production maximum in the hexagonal lattice of Figure 1, and in the case of $N = 8$ which is not shown.

Step 4c of the mechanism of Scheme 1 shows the production of CO* particles, which are responsible for the poisoning almost exclusively with superficial carbon monoxide at even higher $y_{O_2}$ values. This causes an interesting discontinuity in the phase diagram, certainly close to a first order kinetic phase transition that coincides with a sudden growth to high values of $k$ on the ($k$, $y_{O_2}$) curve.

The evolution of the system to absorbent states is well described by eq 3, whose parameter $k$, as commented above, allows a description of the adsorbed phase that is coherent with the behavior of the phase diagram and with the images shown by the snapshots of the MC simulations. This temporary evolution, however, does not fit in the same way with eqs 4 and 5. This situation can be seen in Figure 5, which shows, for two representative oxygen pressures, the linearized diagrams of the three equations using the same range of points obtained in the simulations, with their respective correlations.

## Conclusion

In a complex system of surface reactions, such as the oxidation of $CH_4$, an evolution is seen, determined by MC simulations, to an absorbent phase in the hexagonal ($N = 6$) and $N = 8$ lattices in a narrow zone corresponding to high $O_2$ pressures, and for $N = 4$ over almost the whole range of the phase diagram. This temporal evolution is well described by an exponential decay of production of the form $e^{-kt}$, with a poor fit for other expressions used in the literature. Parameter $k$ allows an adequate description of the system's reactive and absorbent states coherent with the configurations shown by the phase diagram. In the case of a square lattice, over most of the range of concentrations of the gas-phase it is seen that the absorbent configuration of the adsorbed phase complies with the checkerboard structure found by Brosilow and Ziff in the case of a simple mechanism of the CO–NO reaction over a square lattice.

The financial support of this work by FONDECYT under project 1070351 is gratefully acknowledged.

## References

1 G. Nicolis, Y. Prigogine, *Self-Organization in Nonequilbrium Systems*, Wiley Interscience, New York, **1977**; H. Haken, *Synergetics*, Springer-Verlag, New York, **1977**; J. Marro, R. Dickman, *Nonequilibrium Phase Transitions in Lattice Models*, Cambridge University Press, Cambridge, **1999**.

2 D. ben-Avraham, S. Redner, D. B. Considine, P. Meakin, *J. Phys. A: Math. Gen.* **1990**, *23*, L613; D. ben-Abraham, D. B. Considine, P. Meakin, S. Redner, H. Takayasu, *J. Phys. A: Math. Gen.* **1990**, *23*, 4297.

3 R. M. Ziff, E. Gulari, Y. Barshad, *Phys. Rev. Lett.* **1986**, *56*, 2553.

4 B. J. Brosilow, R. M. Ziff, *J. Catal.* **1992**, *136*, 275.

5 B. Meng, W. H. Weinberg, J. W. Evans, *Phys. Rev. E* **1993**, *48*, 3577.

6 K. Yaldram, M. A. Khan, *J. Catal.* **1991**, *131*, 369.

7 J. Cortés, E. Valencia, *Phys. Rev. E* **2003**, *68*, 016111.

8 K. C. Taylor, *Catal. Rev.* **1993**, *35*, 457; M. Shelef, G. W. Graham, *Catal. Rev.* **1994**, *36*, 433; L. F. Razon, R. A. Schmitz, *Catal. Rev.* **1986**, *28*, 89.

9 D. R. Rainer, M. Koranne, S. M. Vesecky, D. W. Goodman, *J. Phys. Chem. B* **1997**, *101*, 10769.

10 Y. Ozawa, Y. Tochihara, M. Nagai, S. Omi, *Chem. Eng. Sci.* **2003**, *58*, 671; P. Hurtado, S. Ordóñez, H. Sastre, F. Díaz, *Appl. Catal., B* **2004**, *47*, 85.

11 J. Cortés, E. Valencia, P. Araya, *Catal. Lett.* **2006**, *112*, 121.

12 V. P. Zhdanov, P.-A. Carlsson, B. Kasemo, *J. Chem. Phys.* **2007**, *126*, 234705.

13 T. V. Choudhary, S. Banerjee, V. R. Choudhary, *Appl. Catal., A* **2002**, *234*, 1; P. Gélin, M. Primet, *Appl. Catal., B* **2002**, *39*, 1; D. Ciuparu, M. R. Lyubovsky, E. Altman, L. D. Pfefferle, A. Datye, *Catal. Rev.* **2002**, *44*, 593.

14 P. Mars, D. W. van Krevelen, *Chem. Eng. Sci.* **1954**, *3*, 41.

15 K. Fujimoto, F. H. Ribeiro, M. Avalos-Borja, E. Iglesia, *J. Catal.* **1998**, *179*, 431; J. Au-Yeung, K. Chen, A. T. Bell, E. Iglesia, *J. Catal.* **1999**, *188*, 132.

16 J. Cortés, H. Puschmann, E. Valencia, *J. Chem. Phys.* **1996**, *105*, 6026; J. Cortés, H. Puschmann, E. Valencia, *J. Chem. Phys.* **1998**, *109*, 6086; E. Valencia, J. Cortés, *Surf. Sci.* **2000**, *470*, L109; J. Cortés, E. Valencia, *Physica A* **2002**, *309*, 26.

17 V. Fried, H. F. Hameka, U. Blukis, *Physical Chemistry*, MacMillan Publishing Co., Inc., New York, **1977**.

18 H. V. Maat, L. Moscou, Proc. 3rd Int. Congr. Catal., North-Holland, Amsterdam, **1965**, p. 1277; A. F. Ogunye, W. H. Ray, *Ind. Eng. Chem. Process Des. Dev.* **1971**, *10*, 410.

19 V. W. Weekman, Jr., *Ind. Eng. Chem. Process Des. Dev.* **1968**, *7*, 90; A. F. Ogunye, W. H. Ray, *Ind. Eng. Chem. Process Des. Dev.* **1970**, *9*, 619.

20 J. W. Evans, *Langmuir* **1991**, *7*, 2514; J. W. Evans, M. S. Miesch, *Phys. Rev. Lett.* **1991**, *66*, 833; P. Meakin, D. J. Scalapino, *J. Chem. Phys.* **1987**, *87*, 731.

21 J. W. Evans, T. R. Ray, *Phys. Rev. E* **1993**, *47*, 1018.

22 J. Cortés, E. Valencia, G. Aguila, E. Orellana, P. Araya, *Catal. Lett.* **2008**, *126*, 63.